Pharm Res (2012) 29:3180–3187
DOI 10.1007/s11095-012-0813-6

RESEARCH PAPER

Pharmacokinetics and Pharmacodynamics of Anti-BR3 Monoclonal Antibody in Mice

Anshu Marathe • Suhasini Iyer • Zhihua Julia Qiu • Jennifer Visich • Donald E. Mager

Received: 13 December 2011 / Accepted: 20 June 2012 / Published online: 18 July 2012

ABSTRACT

Purpose To characterize the pharmacokinetic (PK) and pharmacodynamic (PD) properties of a monoclonal antibody directed against the B-cell activating factor (BAFF) receptor 3 (BR3), following intravenous (IV) and subcutaneous (SC) administration in mice.

Methods Single IV doses of 0.2, 2.0 and 20 mg/kg and a single SC injection of 20 mg/kg of anti-BR3 antibody was administered to mice. Serum drug and BAFF concentrations and splenic B-cell concentrations were measured at various time points. Pooled PK profiles were described by a two-compartmental model with time-dependent nonlinear elimination, and BAFF profiles were defined by an indirect response model. Fractional receptor occupancy served as the driving function for a competitive reversible antagonism model to characterize B-cell dynamics.

Results Noncompartmental analysis revealed a decrease in drug clearance (31.3 to 7.93 mL/day/kg) with increasing IV doses. The SC dose exhibited slow absorption (T_{max}=2 days) and complete bioavailability. All doses resulted in a dose-dependent increase in BAFF concentrations and decrease in B-cell counts. The proposed model reasonably captured complex PK/PD profiles of anti-BR3 antibody after IV and SC administration.

Conclusions A mechanistic model was developed that describes the reversible competition between anti-BR3 antibody and BAFF for BR3 receptors and its influence on B-cell pharmacodynamics.

KEY WORDS B-cell activating factor · B-cell activating factor Receptor 3 · mathematical modeling · pharmacodynamics · pharmacokinetics

INTRODUCTION

Therapies targeting B cells are currently in clinical development for a variety of autoimmune diseases and hematological malignancies. Rituximab, an anti-CD20 monoclonal antibody (Genentech, South San Francisco, CA; Biogen-IDEC, Cambridge, MA; Roche, Basel, Switzerland) effectively produces B cell depletion through antigen- dependent cell-mediated cytotoxicity (ADCC), complement-mediated cytotoxicity (CDC) and apoptosis. Success of this drug in the treatment of non-Hodgkin's lymphoma has given impetus to investigation of novel targets directed towards B cell depletion (1–5).

A key component for the survival of mature B cells is B cell activating factor (BAFF), a protein belonging to the tumor necrosis factor (TNF) family. BAFF binds to three receptors of the TNF family, BR3 (BAFF receptor 3), TACI (transmembrane activator and calcium modulator and cyclophylin ligand interactor) and BCMA (B cell maturation antigen) (1,6). Among these, the BAFF/BR3 interaction is most critical for survival signaling in B cells by upregulation

Electronic supplementary material The online version of this article (doi:10.1007/s11095-012-0813-6) contains supplementary material, which is available to authorized users.

A. Marathe • D. E. Mager (✉)
Department of Pharmaceutical Sciences
University at Buffalo, State University of New York
431 Kapoor Hall
Buffalo, New York 14214, USA
e-mail: dmager@buffalo.edu

S. Iyer • Z. J. Qiu • J. Visich
Genentech Inc.
South San Francisco, California, USA

of anti-apoptotic molecules (7,8). BAFF and BR3 knockout mice show significant loss in peripheral B cells while overexpression of BAFF leads to symptoms associated with autoimmune diseases. Increased levels of BAFF is observed in patients with rheumatoid arthritis, Sjorgen syndrome and systemic lupus erythematosus (6–10). BAFF also promotes B cell metabolic fitness and prepares them for antigen-induced proliferation (11). Thus, strategies for blocking BAFF are currently under investigation. Belimumab (LymphoStat-B; Human Genome Sciences, Rockville, MD) a monoclonal antibody and BR3-Fc (Genentech, South San Francisco, CA; Biogen-IDEC, Cambridge, MA), a fusion protein that binds to BAFF, block the BAFF-BR3 signaling pathway and have shown promising results in non-human primates (12,13).

Antibodies directed against the BR3 receptor are being developed that utilize a dual mechanism of action for B cell depletion. These antibodies bind to the BR3 receptor with high affinity and block BAFF/BR3 binding, thus inhibiting the BR3 survival signaling pathway. In addition to this competitive reversible antagonism, antibodies are also engineered to induce cell killing via Fc-mediated cytotoxicity, thereby incorporating the features of both anti-CD20 antibodies and BR3-Fc proteins in one compound. Mice treated with such antibodies show significantly larger B cell depletion in certain subsets and qualitatively distinct outcomes compared to BR3-Fc or anti-CD20 treated mice (14,15).

The PK/PD analyses of anti-BR3 antibody using quantitative modeling approaches have not been reported. The purpose of this study is to characterize the pharmacokinetics of an anti-BR3 antibody over a range of dose levels in mice. The time course of BAFF is characterized using an indirect response model. A mechanistic competitive reversible antagonism model that simultaneously utilizes the drug and BAFF concentrations is developed to characterize the time course of B cell dynamics.

MATERIALS AND METHODS

Study Design and Bioassay

Single IV doses of 0.2, 2.0 and 20 mg/kg and a single SC injection of 20 mg/kg of anti-BR3 antibody was administered to 4 groups of BALB/c mice. There were 12 animals each in the 0.2 and 2 mg/kg dose groups, and 18 animals each in the 20 mg/kg IV and SC dose groups. Blood samples for PK and BAFF analysis were collected at the following timepoints: 0.0833, 0.5, 2, 4, 8 and 24 h on day 1 and at 2, 4, 7, 10, 14, 17, 21, 28, 36, 56, 63, 73, 77, 85, 92 100, 109 and 119 days post-dose. A staggered sampling strategy was used such that each mouse was bled a total of 3 times, once each using retro-orbital eye bleeds, followed by a terminal bleed at necropsy. Balb/c mice were purchased from Charles River labs. All protocols were reviewed and approved by the Genentech IACUC committee, and all studies were conducted at Genentech.

The serum concentrations of anti-BR3 antibody and BAFF were determined using Enzyme Linked Immuno-Sorbent Assay (ELISA). In brief, for the measurement of anti-BR3 antibody concentration, recombinant human BR3 extracellular domain (ECD) (Genentech) was coated on 96-well microplate plates and goat anti-human IgG conjugated to horseradish peroxidase (HRP) was used as the detection. The minimum dilution of serum samples was 1/100, and the standard curve range was 0.5−32 ng/mL. The minimum quantifiable concentration of anti-BR3 antibody was 75 ng/mL. To determine serum concentrations of BAFF, anti-recombinant human BAFF (rhBAFF) monoclonal antibody A (Genentech) was coated on 96-well microplate plates, and Biotin-conjugated anti-rhBAFF monoclonal antibody B (Genentech) and HRP-Streptavidin (Amdex; Amersham Pharmacia Biotech, Piscataway, NJ) were used as the detection. The minimum dilution of the serum sample was 1/20, and the standard curve range was 3.1−200 pg/mL. The minimum quantifiable concentration of BAFF was 100 pg/mL using rhBAFF as a relative standard. For both assays, three matrix controls containing low, middle, or high concentration of the analyte within the standard curve range were assessed for accuracy and precision during assay development. The overall percentage coefficient of variation (CV) of inter- and intra-assay precision was under 20% for the anti-BR3 antibody assay and under 30% for the BAFF assay. The accuracies of the anti-BR3 antibody and BAFF assays were within 80–120% and 70–130%, respectively.

B cell counts in the spleen were measured at pre-dose, 0.5, 2, 4 and 24 h on day 1 and at 4, 7, 14, 21, 28, 36, 42, 49, 109 and 119 days post-dose. Spleens from three mice per time point per group were collected (terminal time points) and single-cell suspensions were prepared for B cell analysis. FACS analysis of total B cell ($B220^+$) count was conducted on a FACSCalibur™ (Becton-Dickinson; Sunnyvale, CA) with flurochrome conjugated anti-mouse B220 antibody (13).

PK/PD Model

A non-compartmental analysis was conducted to ascertain whether anti-BR3 antibody exhibited linear or non-linear pharmacokinetic properties and thereby aid the model building process. Several pharmacokinetic models were evaluated according to standard model fitting criteria, and the time-course of serum anti-BR3 antibody was ultimately characterized using a two-compartmental model with Michaelis-Menten kinetics (Fig. 1). Drug in the central compartment undergoes linear distribution to a non-specific

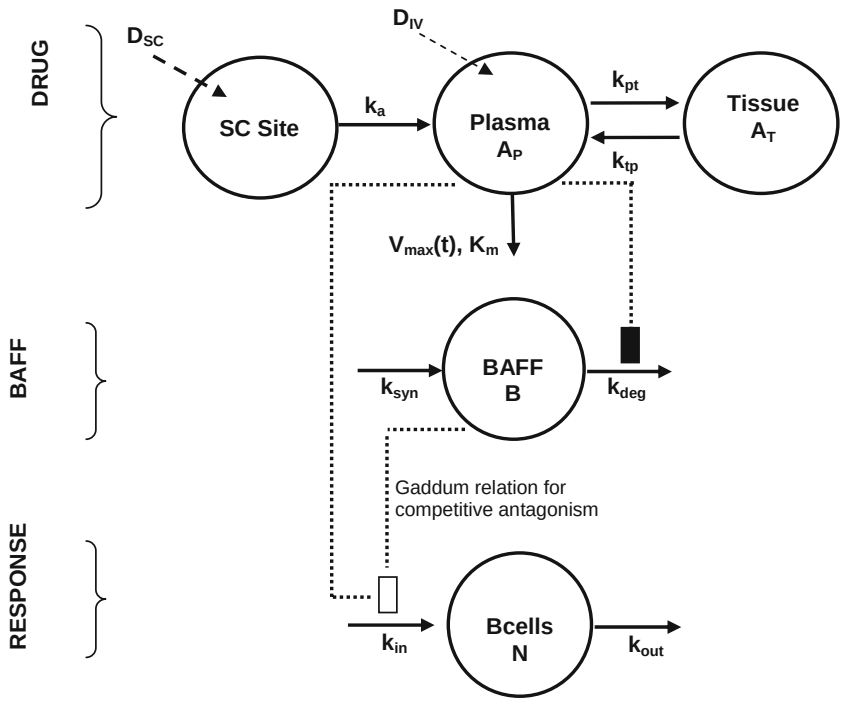

Fig. 1 Competitive reversible antagonism PK/PD model for anti-BR3 monoclonal antibody after IV and SC administration in mice. Drug upon administration into the central compartment (A_p, V_c) after IV dosing or after being absorbed from the subcutaneous site (k_a) after SC dosing undergoes nonlinear elimination (V_{max}, K_m) and linear distribution (k_{pt}, k_{tp}) to a non-specific peripheral compartment (A_T). The turnover of BAFF is described by synthesis (k_{syn}) and degradation (k_{deg}) rate constants with drug inhibiting its degradation. B cell turnover is described by production (k_{in}) and loss (k_{out}) rate constants with occupancy of BR3 receptors stimulating production. Detailed equations are provided in the *PK/PD Model* section of *Materials and Methods*.

peripheral compartment and non-linear elimination, which was suggested by the non-compartmental analysis (see Results). The drug is directly administered into the central compartment with IV dosing, whereas it is absorbed from the subcutaneous injection site by a first-order rate process (k_a) with SC dosing. The equations used to describe the pharmacokinetics are as follows:

$$\frac{dA_p}{dt} = In(t) - \frac{V_{\max}}{K_m + (A_p/V_c)} \cdot (A_p/V_c) - k_{pt} \cdot A_p + k_{tp} \cdot A_T \quad (1)$$

$$\frac{dA_T}{dt} = k_{pt} \cdot A_p - k_{tp} \cdot A_T \quad (2)$$

where A_P and A_T are the amounts of the drug in the central and peripheral compartments, V_c is the volume of the central compartment, k_{pt} and k_{tp} are the first-order rates of distribution between the compartments, V_{max} is the maximal zero-order elimination rate constant, and K_m represents the affinity of the antibody for the target receptor. $In(t)$ is 0 for IV dosing and equal to $Fk_aD_{sc}\exp(-k_at)$ for SC administration, where F is the bioavailability of the drug. V_{max} is assumed to be a time dependent function for the lower doses (0.2 and 2.0 mg/kg):

$$V_{\max} = V_{\max 1} + \frac{E_{\max} t^n}{ET_{50}^n + t^n} \quad (3)$$

where V_{max1} is the zero-order elimination rate constant at t=0. It is assumed that the capacity increases with time and saturates at a value of $V_{max1} + E_{max}$ for longer times. The ET_{50} is the time at which there is 50% of the maximal increase in capacity, and n is the Hill coefficient. This assumption was needed to characterize the pharmacokinetic data and could represent an increase in capacity due to receptor up-regulation. A time-dependent V_{max} function was also applied for the highest dose, but it failed to improve model fitting criteria and also worsened model fitted profiles. Thus, for the highest dose, it was determined that the capacity remains constant at V_{max1}. The initial condition for Eq. 1 was set to 0 for SC and equal to the dose administered for IV dosing. The initial condition for Eq. 2 was set to 0 for both routes of administration.

BAFF dynamics was described by a basic indirect response model (Fig. 1) (16,17). This model assumes that anti-BR3 monoclonal antibody has an inhibitory action on the degradation rate of BAFF, possibly due to competitive inhibition of receptor mediated clearance of BAFF. The rate of change of BAFF over time was defined as:

$$\frac{dB}{dt} = k_{syn} - k_{\deg} \cdot \left(1 - \frac{I_{\max} \cdot C_p}{IC_{50} + C_p}\right) \cdot B \quad (4)$$

where B is the concentration of BAFF in the serum, C_P (=A_P/V_c) is the free drug concentration in the central compartment, k_{syn} is the apparent zero-order production rate of BAFF, k_{deg} is the first-order rate constant of degradation or loss, I_{max} is the maximal fractional extent of inhibition, and IC_{50} is the drug concentration producing 50% of maximal inhibition. The initial condition for Eq. 4 was set to the steady state baseline value of BAFF (B_{SS}), which is the ratio of k_{syn} and k_{deg} ($B_{SS} = k_{syn}/k_{deg}$).

B-cell dynamics in the spleen was described by a competitive reversible antagonism model as both BAFF (agonist) and anti-BR3 (antagonist) bind reversibly to the alpha-BR3 receptor (Fig. 1). Splenic B-cells were assumed to be more therapeutically relevant and utilized for modeling. B-cell data in the peripheral blood were found to be highly variable and not useful for model building purposes (data not shown). It is assumed that BAFF and drug compete for the same target site on the receptor. Such competitive antagonism can be described by a relation that was derived by Gaddum (18,19) for rapid-binding, equilibrium conditions:

$$\rho = \frac{B}{B + K_B \cdot \left(1 + C_p / K_D\right)} \tag{5}$$

with ρ representing the fractional occupancy of the alpha-BR3 receptor by BAFF, and K_B and K_D are the apparent equilibrium dissociation constants of BAFF and the drug. The fractional occupancy is defined as the ratio of the concentrations of BAFF-BR3 receptor complex and the total BR3 receptors (free and bound), where the bound species would include the receptors bound to both BAFF and the drug. The Gaddum relation suggests that increasing concentrations of the drug would decrease receptor occupancy. The pharmacodynamic model assumes that the response is a function of receptor occupancy, and the rate of change of B-cells over time was defined as:

$$\frac{dN}{dt} = k_{in} \cdot \rho - k_{out} \cdot N \tag{6}$$

where N is number of B cells represented by absolute B220 counts, k_{in} is the apparent zero-order production rate, and k_{out} is the first-order rate constant of loss of B-cells. B220 is an isoform of CD45R with a molecular weight of 220 kDa and is an established surface marker predominantly found on B cells. This equation suggests a decrease in the receptor occupancy would result in a decrease in the production of B cells. The initial condition for Eq. 6 was set to the steady state baseline value of B-cells (N_{SS}).

Data Analysis

The two-compartmental model with Michaelis-Menten kinetics (Fig. 1; Eqs. 1–3) was fitted to pooled anti-BR3 monoclonal antibody serum concentration-time profiles. The PK parameters to be estimated included: k_a, k_{pt} (= k_{tp}), V_c, K_m, V_{max1}, E_{max}, and ET_{50}. The bioavailability F was fixed to 1 based on the calculations from non-compartmental analysis. The value of the Hill coefficient (n) was also fixed to 5 to account for the sharp decline in concentrations as revealed by the lower two doses.

The indirect response model (Fig. 1; Eq. 4) was fitted to the pooled BAFF serum concentration-time profiles. The parameters that were estimated included k_{deg}, I_{max}, IC_{50}, and Bss. The PK parameters were fixed in the model, and the production rate, k_{syn}, was calculated to maintain steady-state baseline conditions ($k_{syn} = k_{deg} B_{SS}$). The molecular weight of BAFF was used in the calculation of receptor occupancy and to obtain BAFF concentration in molar units. All modeling was conducted in molar units and then output concentrations were converted to units of the analytical assay. The molecular weight of BAFF was measured to be 51 kDa (data not shown), which is in good agreement with reported values (20–22).

The competitive reversible antagonism PD model (Fig. 1; Eqs. 5–6) was fitted to the pooled spleen B-cell concentration-time profiles. The parameters k_{out}, N_{ss}, K_B and K_D were estimated, whereas the PK and the BAFF profiles were fixed. Similar to BAFF turnover, k_{in} was calculated to maintain steady-state baseline conditions ($k_{in} = k_{out} \cdot N_{SS} / \rho_{SS}$).

All fittings were performed using the ADAPT5 (beta-version) computer program (23) by the maximum likelihood estimation method. The variance model was defined as:

$$VAR_i = \left(\sigma_1 + \sigma_2 \cdot Y_i\right)^2 \tag{7}$$

where VAR_i is the variance of the i^{th} data point, σ_1 and σ_2 are the variance parameters, and Y_i is the model predicted concentration or response. Separate variance models were used by fixing σ_1 to 0.0001 and 0 for PK and PD data. The goodness of fit was assessed by system convergence, Akaike Information Criterion, Schwarz Criterion, examination of residuals, and visual inspection of the fitted curves.

RESULTS

Pharmacokinetics

Non-compartmental analysis of the mean pharmacokinetic data revealed a dose related decrease in the total clearance (CL) of the drug for increasing IV dose levels suggesting non-linear disposition (Table I). The steady state volume of distribution (V_{ss}) of the drug also showed a decrease with increasing dose, with V_{ss} of the intermediate dose being atypically low. The terminal half-life and mean residence time (MRT) increases with dose. For SC dosing, the maximum plasma concentration (C_{max}) occurs at 2 days (T_{max}) post-dose. The drug exhibits complete bioavailability with a calculated apparent value of 1.28.

The pooled serum concentration-time profiles of anti-BR3 monoclonal antibody and fitted curves after three single IV doses and a single SC dose in mice are shown in Fig. 2. The profiles show a polyexponential behavior and slow absorption for the SC dosing. The proposed two-

Table I Noncompartmental Analysis of Anti-BR3 Monoclonal Antibody Pharmacokinetics in Mice

Dose (mg/kg)	$T_{1/2}$[#] (day)	C_{max} (μg/mL)	T_{max} (day)	AUC (μg·day/mL)	CL or CL/F[*] (mL/day/kg)	V_{SS} or V_{SS}/F[*] (mL/kg)	MRT (day)
0.2 iv	3.13	3.67	–[a]	6.38	31.3	99.3	3.17
2 iv	2.62	39.9	–[a]	115	17.4	60.9	3.50
20 iv	7.37	509	–[a]	2523	7.93	77.1	9.73
20 sc	8.56	313	2.0	3219	6.21[*]	75.7[*]	12.2

[#] Represents terminal half-life

*For SC dosing the clearance (CL/F) and steady state volume of distribution (Vss/F) are adjusted for bioavailability

[a] Not applicable

compartmental model with Michaelis-Menten kinetics and a time dependent V_{max} for the lower two doses characterized the plasma concentrations of the drug reasonably well. A time-dependent V_{max} was needed to account for the sharp decline in plasma concentrations for the lower two doses. This could suggest an increased binding capacity due to receptor up-regulation. The final estimated parameters are listed in Table II and low CV% values were obtained. Initial estimates of k_{tp} and k_{pt} were similar, and the two rate constants were assumed to be the same to reduce the number of parameters in the model and increase the precision of the final estimated parameters. The estimated volume of the central compartment (0.0551 L/kg) is approximately equal to the plasma volume of mice. The bioavailability (F) was fixed to 1 in the model based on the non-compartmental analysis (NCA) results. The calculated apparent value of bioavailabilty from NCA is 1.28, and the reasonable fit of the final model to the data further supports the assumption of complete bioavailabilty. The value of the Hill coefficient (n) for the time-dependent V_{max} function was fixed to 5 to reflect a sharp concentration-effect relationship based on preliminary runs where estimation of n resulted in large values and CV%. The model predicts the concentration-time profiles reasonably well; however, even with the time dependent increase in V_{max}, the concentrations were over-predicted for the 2.0 mg/kg dose in the terminal phase. An alternative model with a time-dependent decrease in V_{max} for the highest dose level, instead of a time-dependent increase for the lower doses, was also tested. The model fits were comparable to the proposed model (Figure S1 in supplementary materials). These modeling efforts suggest either an up-regulation of the receptor for lower doses or receptor down-regulation for the highest dose level. Thus, it is difficult to distinguish between these two processes with the given data. Clearly additional experiments would be needed to test these hypotheses and understand the complicated pharmacokinetics of anti-BR3 monoclonal antibody. In the absence of further experimental evidence to support either process, the proposed PK model with a time-dependent increase in V_{max} for the lower doses was used for fitting the pharmacodynamic markers of anti-BR3 antibody exposure.

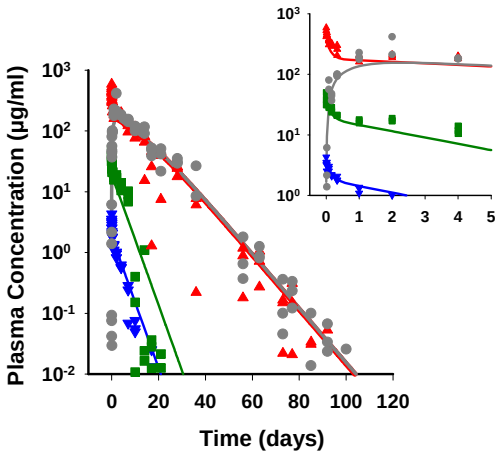

Fig. 2 Pharmacokinetic profiles of anti-BR3 monoclonal antibody after simultaneously fitting the pharmacokinetic model to pooled data of three single IV doses of 0.2 (blue inverted triangle), 2.0 (*green square*), 20 mg/kg (*red triangle*), and a single SC dose of 20 mg/kg (*gray circle*). Symbols represent experimental data and lines represent model-fitted profiles. The inset shows data and profiles for initial time points.

Pharmacodynamics

The time-course of the pooled concentrations of BAFF in serum, B-cells in spleen and their fitted curves after three single IV doses and a single SC dose in mice are shown in Fig. 3. The overall BAFF profile shows an increase in concentration, which can be attributed to a decrease in receptor

Table II Pharmacokinetic Parameter Estimates for Anti-BR3 Monoclonal Antibody in Mice

Parameter (units)	Final Estimate	CV%
k_a (day^{-1})	1.33	12.6
k_{pt}, k_{tp} (day^{-1})	3.84	14.6
V_c (L/kg)	0.0551	4.99
K_m (μM)	1.28	19.4
V_{max1}(μmole/kg/day)	0.0148	15.4
E_{max}(μmole/kg/day)	0.0217	20.7
ET_{50} (day)	0.37	13.5

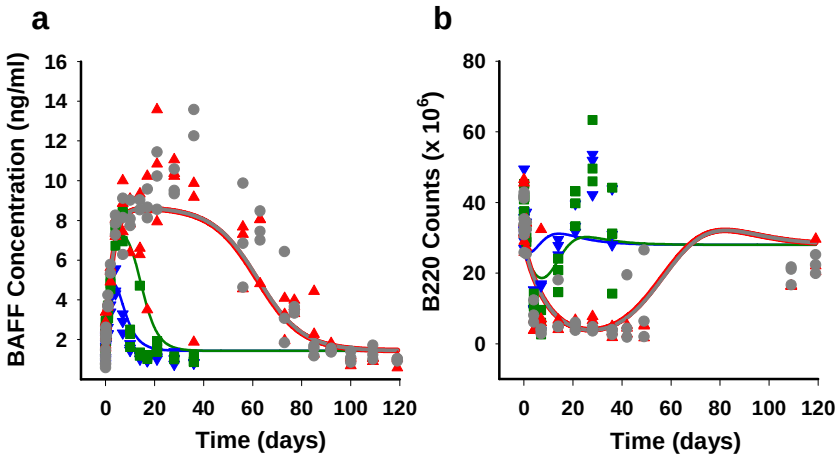

Fig. 3 Concentration-time profiles of (**a**) BAFF in serum and (**b**) B-cells in spleen after simultaneously fitting the pharmacodynamic model to pooled data for three single IV doses of 0.2 (*blue inverted triangle*), 2.0 (*green square*), 20 mg/kg (*red triangle*), and a single SC dose of 20 mg/kg (*gray circle*) of anti-BR3 monoclonal antibody. BAFF and B-cell concentrations were fitted sequentially. Symbols represent experimental data and lines are model-fitted profiles.

mediated clearance as a result of binding of the drug to BR3 receptors. This is followed by a smooth decline in concentrations to baseline as the drug is washed out from the system. The indirect response model reasonably captures the time-course of BAFF concentrations (Fig. 3a), and low CV% values were obtained for the final estimated parameters (Table III). There was significant variability in the data, and peak concentrations for the highest dose (IV and SC) were under predicted. The concentration is over predicted for the 0.2 and 2 mg/kg dose during the return phase which is reflective of the over prediction in the PK driving function.

The overall B-cell profiles show a decline due to the inhibition of BAFF-BR3 binding caused by the anti-BR3 antibody. A subsequent increase in B220 counts to baseline is observed as the antibody is cleared. The competitive reversible antagonism model describes the pharmacodynamic data reasonably well especially the 20 mg/kg IV and SC doses (Fig. 3b). However, this model does not capture the apparent rebound phenomena observed only for the lower two dose levels in this study. Such rebound phenomena were not observed for similar studies conducted in monkeys and humans (data not shown). The final estimated parameters are listed in Table III, and low CV% values were obtained for all but one (K_B) of the fitted parameters.

Table III Pharmacodynamic Parameter Estimates for Anti-BR3 Monoclonal Antibody in Mice

Parameter (units)	Final Estimate	CV%
BAFF dynamics		
k_{deg} (day^{-1})	2.18	14.1
IC_{50} (nM)	0.991	16.3
I_{max} (dimensionless)	0.835	1.2
B_0 (ng/mL)	1.43	4.07
B-cell dynamics		
k_{out} (day^{-1})	0.101	8.88
N_0 (x 10^6)	28.0	5.57
K_B (nM)	0.0603	122
K_D (nM)	2.72	33.4

One explanation for the high CV% for K_B is that the concentration range for BAFF is relatively limited and may influence the ability to estimate the parameter reliably. The estimated value of the apparent equilibrium dissociation constant of BAFF (K_B) was 0.0603 nM and is consistent with an estimate (~0.1 nM) reported in the literature (24). Similarly, the estimated apparent equilibrium dissociation constant of 2.72 nM for the anti-BR3 antibody (K_D) lies within the range of values (0.6–7.9 nM) obtained experimentally (14).

The simulated occupancy of the BR3 receptor by BAFF shows a sharp decline in the receptor occupancy and subsequent return to baseline (Fig. 4). A slight rebound phenomenon is observed for all four profiles, suggestive of increased occupancy due to elevated levels of BAFF in the serum which binds to the BR3 receptors after the drug is removed from the system. The model predicts the steady state baseline value of occupancy to be 0.318 implying that at steady state only 31.8% of the BR3 receptors are occupied by the agonist. The occupancy declines

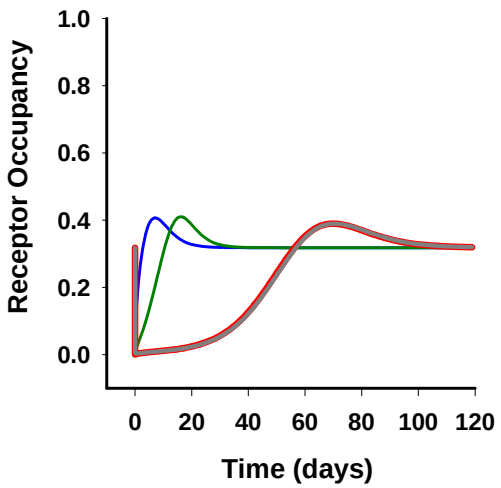

Fig. 4 Simulated occupancy of the BR3 receptor using the competitive reversible antagonism PK/PD model for three single IV doses of 0.2 (*blue*), 2.0 (*green*), 20 mg/kg (*red*), and a single SC dose of 20 mg/kg (*gray*) of anti-BR3 monoclonal antibody.

to approximately 0 (less than 1%) for the 2 and 20 mg/kg doses suggesting that all BAFF is displaced from the receptor by the antibody.

DISCUSSION

The primary objective of this study was to characterize the pharmacokinetic and pharmacodynamic profiles of anti-BR3 monoclonal antibody using a mechanism based model. To this end, the pharmacokinetics of the drug was described by a two compartmental model with non-linear elimination, and the concentration-time profiles of BAFF, the natural ligand of the BR3 receptors, were described by an indirect response model. A mechanism-based competitive reversible antagonism model was used to describe the time course of B cells in spleen (Fig. 1). Considering the complexity of the preclinical profiles, this model adequately described the experimental data (Figs. 2 and 3). In addition, the PK/PD model not only describes the plasma concentrations of the antibody, but also its natural ligand, and subsequently translates both to occupancy of the pharmacological target in order to drive the pharmacodynamic response. This represents a fundamental approach to model the mechanism of action of antibodies and is not only pertinent to this study but might be for other antibodies as well. Abciximab competes with endogenous agonists like thrombin for the glycoprotein IIb/IIIa platelet-surface integrin that mediate platelet aggregation (25). Similarly, Cetuximab competes with natural ligands for the epidermal growth factor receptors, thus inhibiting the downstream signals important for growth (26). There are several other examples of antibodies where competitive reversible antagonism is critical (27).

Noncompartmental analysis of the plasma concentration profiles of the anti-BR3 monoclonal antibody showed an apparent trend for decreasing clearance (*CL*) with increasing dose (Table I). The observed relationship between dose and V_{ss} is atypical with the intermediate dose having the lowest V_{ss}. These nonlinear properties might be attributed to saturable binding with BR3 receptors. A time-dependent increase in V_{max} for the lower dose levels was needed to account for the very sharp decline in the pharmacokinetic profile of the drug (Fig. 2). Our preliminary modeling efforts with a time-invariant V_{max} substantially over predicted the concentrations for the lower doses (data not shown). Considering the complexity of the non-linear PK profile, the proposed model adequately described the data. An alternative model that utilized a time-dependent decrease in V_{max} for the highest dose provided comparable fits to the data (Figure S1). Significant depletion of B cells for the highest dose could be partly attributed to the reduction in receptor capacity, as BR3 receptors are present on B cells. Thus, it is difficult to distinguish between such processes and to fully understand the complicated pharmacokinetic behavior of anti-BR3 antibody with the current data. Further experimentation is clearly needed to test these hypotheses. Another model permutation included a linear clearance term added to the proposed clearance model. However, parallel linear elimination failed to significantly improve model performance (data not shown). Thus for parsimony, the proposed model with only non-linear clearance was retained.

The concentration-time profiles of BAFF in the serum were adequately described by an indirect-response model with the drug inhibiting its degradation (Fig. 3a) indicative of a decline in receptor-mediated clearance of the BAFF-BR3 complex. Decrease in receptor mediated clearance has been reported as one of the possible mechanisms for an increase in serum BAFF concentrations in mice lacking B cells or in patients with depleted B cells after rituximab treatment (15,28). This is consistent with target-mediated disposition, and future models might be constructed based on such principles should additional receptor level dynamics become available (29,30).

The Gaddum equation (18,19) was implemented to describe the time course of B-cell concentrations in the spleen (Fig. 3b). It was assumed that the occupancy of the BR3 receptor stimulates the production of B cells (i.e., linear transduction of target occupancy). While there is no evidence that BAFF directly induces B cell proliferation, it is shown that BAFF promotes B cell metabolic fitness and prepares them for antigen-induced proliferation (11). The proposed PD model described the data reasonably well. Inclusion of the Fc-mediated cytotoxic effect in the model did not improve the model fitting criteria and reduced the precision of the estimated parameters (data not shown). Since it is known that BAFF promotes B cell survival by upregulating anti-apoptotic molecules (7), a pharmacodynamic model where the binding of the BAFF and BR3 receptor inhibits the loss of B cells was also conducted. In this model the turnover of B cells was described as $dN/dt = k_{in} - k_{out}N/\rho$. While this model behaved similarly to the proposed model for the highest dose, it significantly under predicted the B cell concentrations for the lower dose levels. Our model focuses on splenic B cells as studies suggest that B cell response in lymphoid tissues better represents the cell population that should be targeted (i.e., slowly recirculating cells) for treating autoimmune diseases and hematologic neoplasms (13,31).

The proposed PD model can potentially predict a rebound in response which is evident from the rebound in the simulated profiles of receptor occupancy (Fig. 4). This rebound suggests increased occupancy when BAFF at high concentrations binds to BR3 receptors as the drug is cleared. Such a rebound is likely to be pronounced in the response profiles for drugs with very high clearance relative to endogenous ligand turnover.

In summary, the current study is the first model-based examination of the pharmacokinetic and pharmacodynamic properties of an anti-BR3 monoclonal antibody. The complex non-

linear disposition of the drug was adequately characterized using a model with time and concentration dependent non-linear clearance. Overall, the proposed pharmacodynamic model is mechanistic in nature reflecting alterations in cellular dynamics due to a reversible competition between the antibody and endogenous ligand for the pharmacological target.

ACKNOWLEDGMENTS AND DISCLOSURES

This research was funded, in part, by NIH grant GM57980 (D.E.M.). Dr. Mager has served as a paid consultant to Genentech Inc.

REFERENCES

1. Browning JL. B cells move to centre stage: novel opportunities for autoimmune disease treatment. Nat Rev. 2006;5:564–76.
2. Castillo J, Winer E, Quesenberry P. Newer monoclonal antibodies for hematological malignancies. Exp Hematol. 2008;36:755–68.
3. Cheson BD, Leonard JP. Monoclonal antibody therapy for B-cell non-Hodgkin's lymphoma. N Engl J Med. 2008;359:613–26.
4. Cvetkovic RS, Perry CM. Rituximab: a review of its use in non-Hodgkin's lymphoma and chronic lymphocytic leukaemia. Drugs. 2006;66:791–820.
5. Silverman GJ, Khanna S. B cell modulation in rheumatology. Curr Opin Pharmacol. 2007;7:426–33.
6. Rolink AG, Melchers F. BAFFled B cells survive and thrive: roles of BAFF in B-cell development. Curr Opin Immunol. 2002;14:266–75.
7. Kalled SL. Impact of the BAFF/BR3 axis on B cell survival, germinal center maintenance and antibody production. Semin Immunol. 2006;18:290–6.
8. Shulga-Morskaya S, Dobles M, Walsh ME, Ng LG, MacKay F, Rao SP, *et al.* B cell-activating factor belonging to the TNF family acts through separate receptors to support B cell survival and T cell-independent antibody formation. J Immunol. 2004;173:2331–41.
9. Kalled SL. The role of BAFF in immune function and implications for autoimmunity. Immunol Rev. 2005;204:43–54.
10. Mackay F, Browning JL. BAFF: a fundamental survival factor for B cells. Nature Reviews. 2002;2:465–75.
11. Patke A, Mecklenbrauker I, Erdjument-Bromage H, Tempst P, Tarakhovsky A. BAFF controls B cell metabolic fitness through a PKC beta- and Akt-dependent mechanism. J Exp Med. 2006;203: 2551–62.
12. Halpern WG, Lappin P, Zanardi T, Cai W, Corcoran M, Zhong J, *et al.* Chronic administration of belimumab, a BLyS antagonist, decreases tissue and peripheral blood B-lymphocyte populations in cynomolgus monkeys: pharmacokinetic, pharmacodynamic, and toxicologic effects. Toxicol Sci. 2006;91:586–99.
13. Vugmeyster Y, Seshasayee D, Chang W, Storn A, Howell K, Sa S, *et al.* A soluble BAFF antagonist, BR3-Fc, decreases peripheral blood B cells and lymphoid tissue marginal zone and follicular B cells in cynomolgus monkeys. Am J Pathol. 2006;168:476–89.
14. Lee CV, Hymowitz SG, Wallweber HJ, Gordon NC, Billeci KL, Tsai SP, *et al.* Synthetic anti-BR3 antibodies that mimic BAFF binding and target both human and murine B cells. Blood. 2006; 108:3103–11.
15. Lin WY, Gong Q, Seshasayee D, Lin Z, Ou Q, Ye S, *et al.* Anti-BR3 antibodies: a new class of B-cell immunotherapy combining cellular depletion and survival blockade. Blood. 2007;110:3959–67.
16. Dayneka NL, Garg V, Jusko WJ. Comparison of four basic models of indirect pharmacodynamic responses. J Pharmacokinet Biopharm. 1993;21:457–78.
17. Sharma A, Jusko WJ. Characteristics of indirect pharmacodynamic models and applications to clinical drug responses. Br J Clin Pharmacol. 1998;45:229–39.
18. Gaddum JH. The quantitative effects of antagonistic drugs. J Physiol. 1937;89:7P–9.
19. Kenakin T. Pharmacologic analysis of drug-receptor interaction. Raven Press. 1993;10:331–73.
20. Schneider P, MacKay F, Steiner V, Hofmann K, Bodmer JL, Holler N, *et al.* BAFF, a novel ligand of the tumor necrosis factor family, stimulates B cell growth. J Exp Med. 1999; 189:1747–56.
21. Shu HB, Hu WH, Johnson H. TALL-1 is a novel member of the TNF family that is down-regulated by mitogens. J Leukoc Biol. 1999;65:680–3.
22. Tribouley C, Wallroth M, Chan V, Paliard X, Fang E, Lamson G, *et al.* Characterization of a new member of the TNF family expressed on antigen presenting cells. Biol Chem. 1999;380: 1443–7.
23. D'Argenio DZ, Schumitzky A, Wang X. ADAPT 5 user's guide. Los Angeles: Biomedical Simulation Resource; 2009.
24. Lesley R, Xu Y, Kalled SL, Hess DM, Schwab SR, Shu HB, *et al.* Reduced competitiveness of autoantigen-engaged B cells due to increased dependence on BAFF. Immunity. 2004;20:441–53.
25. Phillips DR, Charo IF, Scarborough RM. GPIIb-IIIa: the responsive integrin. Cell. 1991;65:359–62.
26. Katzel JA, Fanucchi MP, Li Z. Recent advances of novel targeted therapy in non-small cell lung cancer. J Hematol Oncol. 2009;2:2.
27. Wang W, Wang EQ, Balthasar JP. Monoclonal antibody pharmacokinetics and pharmacodynamics. Clin Pharmacol Ther. 2008;84:548–58.
28. Lavie F, Miceli-Richard C, Ittah M, Sellam J, Gottenberg JE, Mariette X. Increase of B cell-activating factor of the TNF family (BAFF) after rituximab treatment: insights into a new regulating system of BAFF production. Ann Rheum Dis. 2007;66:700–3.
29. Levy G. Pharmacologic target-mediated drug disposition. Clin Pharmacol Ther. 1994;56:248–52.
30. Mager DE. Target-mediated drug disposition and dynamics. Biochem Pharmacol. 2006;72:1–10.
31. Gong Q, Ou Q, Ye S, Lee WP, Cornelius J, Diehl L, *et al.* Importance of cellular microenvironment and circulatory dynamics in B cell immunotherapy. J Immunol. 2005;174:817–26.